KRAS mutation-induced EndMT of brain arteriovenous malformation is mediated through the TGF-β/BMP-SMAD4 pathway

Hongyuan Xu,[1,2] Ran Huo,[1,2] Hao Li,[1,2] Yuming Jiao ![ORCID],[1,2] Jiancong Weng,[1,2] Jie Wang,[1,2] Zihan Yan,[1,2] Junze Zhang,[1,2] Shaozhi Zhao,[1,2] Qiheng He ![ORCID],[1,2] Yingfan Sun,[1,2] Shuo Wang,[1,2] Yong Cao ![ORCID] [1,2,3]

[1]Department of Neurosurgery, Beijing Tiantan Hospital, Capital medical university, Beijing, China
[2]China National Clinical Research Center for Neurological Diseases, Beijing, China
[3]Beijing Neurosurgical Institute, Capital Medical University, Beijing, China

Correspondence to
Dr Yong Cao; caoyong@bjtth.org

ABSTRACT

Objective Somatic KRAS mutations have been identified in the majority of brain arteriovenous malformations (bAVMs), and subsequent in vivo experiments have confirmed that KRAS mutation in endothelial cells (ECs) causes AVMs in mouse and zebrafish models. Our previous study demonstrated that the KRAS^{G12D} mutant independently induced the endothelial-mesenchymal transition (EndMT), which was reversed by treatment with the lipid-lowering drug lovastatin. However, the underlying mechanisms of action were unclear.

Methods We used human umbilical vein ECs (HUVECs) overexpressing the KRAS^{G12D} mutant for Western blotting, quantitative real-time PCR, and immunofluorescence and wound healing assays to evaluate the EndMT and determine the activation of downstream pathways. Knockdown of SMAD4 by RNA interference was performed to explore the role of SMAD4 in regulating the EndMT. BAVM ECs expressing the KRAS^{G12D} mutant were obtained to verify the SMAD4 function. Finally, we performed a coimmunoprecipitation assay to probe the mechanism by which lovastatin affects SMAD4.

Results HUVECs infected with KRAS^{G12D} adenovirus underwent the EndMT. Transforming growth factor beta (TGF-β) and bone morphogenetic protein (BMP) signalling pathways were activated in the KRAS^{G12D}-mutant HUVECs and ECs in bAVM tissue. Knocking down SMAD4 expression in both KRAS^{G12D}-mutant HUVECs and ECs in bAVM tissues inhibited the EndMT. Lovastatin attenuated the EndMT by downregulating p-SMAD2/3, p-SMAD1/5 and acetylated SMAD4 expression in KRAS^{G12D}-mutant HUVECs.

Conclusions Our findings suggest that the KRAS^{G12D} mutant induces the EndMT by activating the ERK-TGF-β/BMP-SMAD4 signalling pathway and that lovastatin inhibits the EndMT by suppressing TGF-β/BMP pathway activation and SMAD4 acetylation.

WHAT IS ALREADY KNOWN ON THIS TOPIC

⇒ Somatic KRAS mutations have been identified in the majority of brain arteriovenous malformations (bAVMs). Meanwhile, the KRAS^{G12D} mutant independently induced the endothelial-mesenchymal transition (EndMT), which was reversed by treatment with the lipid-lowering drug lovastatin. However, the underlying mechanisms of action were unclear.

WHAT THIS STUDY ADDS

⇒ KRAS mutation induced EndMT through the transforming growth factor beta (TGF-β)/bone morphogenetic protein (BMP)-SMAD4 pathways.

⇒ Lovastatin reversed KRAS mutation-induced EndMT by inhibiting the TGF-β/BMP pathways and SMAD4 acetylation.

HOW THIS STUDY MIGHT AFFECT RESEARCH, PRACTICE OR POLICY

⇒ Our study implies that SMAD4 may be a potential target by which to inhibit the development of bAVMs with a KRAS mutant and lovastatin (an FDA-approved drug) might alleviate the development of bAVMs and reduce the risk of bAVMs rupture, which need further animal studies and clinical trials.

INTRODUCTION

Brain arteriovenous malformations (bAVMs) constitute a congenital cerebrovascular disease caused by abnormally dilated vascular tangles and are characterised by a lack of capillary beds, which are important for direct arterial-venous communication.[1] BAVMs may lead to devastating haemorrhages, which account for approximately one-third of primary intracerebral haemorrhages in young adults.[2] Clinical treatments mainly include neurosurgery, embolisation and stereotactic radiotherapy.[3] However, the management of large bAVMs, particularly those located in eloquent cortex areas, remains challenging.

In previous research, somatic KRAS-activating mutations were identified in endothelial cells (ECs) of human sporadic bAVMs.[4 5] Subsequent in vivo experiments confirmed that KRAS mutations could drive abnormal vascular morphology and AVMs in mice and zebrafish models in ECs.[6 7] In our previous study, we found endothelial-mesenchymal transition (EndMT) of cells in bAVM tissue, and KRAS mutation induced the

EndMT.[8] Nevertheless, the mechanism by which KRAS mutants trigger the EndMT is still unclear.

In the EndMT, ECs lose their endothelial markers (von Willebrand factor (VWF) and VE-Cadherin) and obtain mesenchymal or myofibroblastic phenotype to express mesenchymal cell products (N-Cadherin and SLUG).[9] As the EndMT contributes to many diseases, pharmacological modulation of an important signalling pathway for EndMT is prove to be effective therapy.[10] Since the EndMT plays an important role in bAVMs,[8 11] illuminating the mechanism by which the EndMT is induced by KRAS mutations will likely help in the development of novel therapies for bAVMs.

In this study, we delivered KRAS[G12D] into human umbilical vein ECs (HUVECs) using adenovirus to explore the mechanism by which this mutant induces the EndMT. Furthermore, we probed the mechanism by which the lipid-lowering drug lovastatin attenuates the EndMT.

METHODS AND MATERIALS
HUVEC culture and treatment
HUVECs cell lines were purchased from Sciencell (#8000, ScienCell) and cultured in endothelial cell medium (ECM, #1001, ScienCell); no HUVECs cultured after the tenth passage (P10) were used. Inhibitors of MAPK (U0126, 20 µM, Selleck), transforming growth factor beta (TGF-β) (SB525334, 20 µM, Selleck), bone morphogenetic protein (BMP, LDN193189, 0.5 µM, Selleck) and lovastatin (S2061, 10 µM, Selleck) were dissolved with Dimethyl sulfoxide (DMSO) and added were directly to the ECM.

Cell culture of primary bAVM ECs
AVM surgical specimens were obtained from the Department of Neurosurgery at Beijing Tiantan Hospital, Capital Medical University. The ECs of the bAVMs were isolated and cultured according to previously described method.[8] Briefly, the tissue was washed with PBS. After cutting into small cubes, tissue was incubated by 0.1% collagenase (Sigma, USA) at 37°C for 15 min. Predigested tissue was triturated with a 2 mL pipette and filtered through a 100 µm cell strainer (BD, USA). After centrifugation of the cell suspension (300G, 3 min), the cells were washed and resuspended in ECM. ECs were isolated using anti-CD31 Dynabeads (#130-091-935, Miltenyi Biotec).

RNA sequencing (RNA-seq)
RNA-Seq was performed according to protocols described previously.[12] Briefly, measurement libraries were created using the NEBNext Ultra Directional RNA Library Prep Kit (Illumina, USA). The strands of cDNA were synthesised using M-MuLV reverse transcriptase (RNaseH-). PCR was performed with Index (X) Primer, universal PCR primers and Phusion High-Fidelity DNA polymerase. We clustered index-encoded samples with the cBot Cluster Generation System using TruSeq PE Cluster Kit v3-cBot-HS. Finally, the libraries were placed on the Illumina HiSeq platform.

RNA-seq data processing and analysis
Raw data containing adaptors or poly-N and low-quality reads were removed. After that, GC content, Q20 value and Q30 value of clean data were calculated. Records and reference genes were downloaded directly from the genome website. We constructed the index of the reference genome using bowtie2 V.2.2.8, and the paired-end clean reads were aligned to the reference genome using Hisat2 V.2.0.5. Human Genome V.19 (Hg19) RefSeq RNA sequences (GRCh37) were downloaded from the UCSC Genome Browser (http://genome.ucsc.edu), and we aligned clean reads with both the transcript reference and the hg19 reference genome using STARv2.2.1. The gene expression was calculated with RSEM v1.3.0 using fragments per kilobase of exon per million mapped fragment values. Differentially expressed EndMT-related genes were shown in online supplemental table S1. Transcripts showing fold change >1.50 or <0.67, with a p<0.05, were considered as differentially expressed.

DNA extraction and whole-exome sequencing
To isolate genomic DNA from primary ECs, commercially available kits (QIAGEN Gentra Puregene) were used following established protocols. First, DNA degradation and contamination were monitored on 1% agarose gels. Second, the DNA concentration was quantitated by Qubit V.2.0 Fluorometer (Invitrogen, USA) using Qubit DNA Assay Kit. Using an Agilent SureSelect Human All Exon V6 kit (Agilent Technologies, USA), we generated sequencing libraries. The index-coded samples were clustered by cBot Cluster Generation System using an Illumina HiSeq PE Cluster Kit. After that, the DNA libraries were sequenced on an Illumina HiSeq platform, and 150 bp paired-end reads were produced. The generated data were mapped to the UCSC hg19 human genome reference with Burrows-Wheeler Aligner software[13] using the default parameters. Picard was used to mark duplicates, and SAMtools[14] was used to sort the alignments by coordinates. Median coverage was estimated by calculating the depth of autosomal common single-nucleotide polymorphism loci using the multicov function in bedtools. Finally, three cases of ECs with KRAS[G12D] mutation confirmed by WES were randomly selected for subsequent in vitro experiments.

Droplet digital PCR
Approximately 10 ng of fresh-frozen template DNA was used in each reaction. The analysis was performed on a QX200 droplet digital PCR (ddPCR) system (Bio-Rad Laboratories, Hercules, California, USA). A variant was considered positive when the sample displayed at least four positive droplets.

Adenovirus-mediated gene expression
Adenovirus encoding KRAS isoform B (G12D) was designed, constructed and produced by Beijing Syngen-Tech. All adenoviruses were amplified in Ad293 cells, purified using the freeze-thaw method followed by CsCl

density gradient centrifugation. For transient transduction, HUVECs were infected with adenovirus encoding KRAS[G12D] or an EGFP control at a multiplicity of infection of 20 for 48 hours. Finally, the cells were grown in ECM until confluent.

Short interfering RNA (siRNA) transfection
siRNA directed against SMAD4 was used for the knockdown experiments. ECs were transfected with siRNAs using Lipo3000 (Invitrogen). After transfection for 48 hours, the cells were harvested for subsequent mRNA or protein expression analysis. siRNA was synthesised with the following sequences: SMAD4, 5'- CGGUCUUUGUAC AGAGUUAUU-3' and the negative control, 5'-UAAC UCUGUACAAAGACCGUU-3'.

Immunohistochemistry
The histological sections obtained from KRAS[G12D] mutant bAVMs were obtained from our previous study.[8] Briefly, bAVM tissue slices were incubated with primary antibody against p-SMAD2/3 (1:200, #8828; CST) or p-SMAD1/5 (1:200, #9516; CST) overnight. In the next day, slices were incubated with secondary antibody (25°C, 1 hour) and horseradish peroxidase–labelled streptavidin (25°C, 30 min). After washing with Tris buffer for three times, sections were stained with 3,3′-diaminobenzidine, and nuclei were counterstained with haematoxylin. We used a positive fluorescence microscope (Zeiss Axio Scope A1) to acquire images.

Immunofluorescence
For immunofluorescent staining, HUVECs were grown on glass coverslips until confluence, and then 4% paraformaldehyde was used to fixed HUVECs. After permeabilising with 0.3% Triton X-100 and blocking with 10% goat serum, HUVECs were incubated with primary antibodies against VE-Cadherin (1:400, #2500, CST), VWF (1:400, #65707, CST), N-Cadherin (1:200, #13116, CST) and SLUG (1:400, #9585, CST) at 4°C overnight and to Goat Anti-Rabbit IgG H&L (1:500,150077, Abcam) and Goat Anti-Rabbit IgG H&L (1:500, ab150080, Abcam). DAPI staining was used to label cell nuclei. All glass coverslips were imaged using an inverted OLYMPUS IX71 microscope.

Quantitative real-time PCR
Total RNA from HUVECs was isolated using TRIzol reagent (Invitrogen, USA). cDNA was reversely transcribed and amplified using a PrimeScript RT reagent Kit (Takara). PCR was performed using TB Green Premix Ex Taq (Takara) with a QuantStudio 3 System (Applied Biosystems). The relative quantification was determined with 2-DeltaDeltaCt method, and GAPDH was considered as the internal reference gene for normalisation. All primer sequences used in this study are shown in online supplemental table S2.

Coimmunoprecipitation and western blot analyses
HUVECs were lysed with radioimmunoprecipitation assay lysis buffer (Sigma, USA), and a bicinchoninic

acid (BCA) protein assay kit (Sigma, USA) was used to detect protein concentration. For Western blot, different samples with an equal amount of protein (20 μL) were loaded into sodium dodecyl sulfate–polyacrylamide gel electrophoresis for electrophoresis and followed by transferring to a polyvinylidene fluoride transfer membrane. The electrochemiluminescence (ECL) reagent was used for visualisation of protein signals, and the grey values of bands were quantified with ImageJ (National Institutes of Health (NIH) Image, Bethesda, MD). The detailed information of antibodies used are as follow: anti-VE-Cadherin (1:1000, #2500, CST), anti-VWF (1:1000, #65707, CST), anti-N-Cadherin (1:1000, #13116, CST), anti-SLUG (1:1000, #9585, CST), anti-SMAD4 (1:1000, #46535, CST), anti-ERK1/2 (1:1000, #4695, CST), anti-p-ERK1/2 (1:2000, #4370, CST), anti-AKT (1:1000, #4685, CST), anti-p-AKT (1:2000, #4060, CST), anti-P38 (1:1000, #8690, CST), anti-p-P38 (1:1000, #4511,CST), anti-p-SMAD2/3 (1:1000, 8828, CST), anti-SMAD2/3 (1:1000, 8685, CST), anti-p-SMAD1/5 (1:1000, 9516, CST), anti-SMAD1/5/9 (1:1000, ab80255, Abcam), anti-β-catenin (1:1000, 8480, CST), anti-SIRT1 (1:1000, 8469, CST), Acetylated-Lysine Antibody (1:1000, 9441, CST), anti-GAPDH (1:1000, #5174,CST).

Coimmunoprecipitation was carried out by using a Protein A/G immunoprecipitation kit (Solarbio). HUVEC lysates were incubated with an anti-SMAD4 antibody (1:200, #46535, CST), followed by incubation with Pierce Protein A/G magnetic beads. The protein eluates were blotted with anti-SMAD4 and anti-acetylated lysine antibodies (1:1000, #9441, CST).

Wound healing assay
Wound healing assays were performed using an Ibidi culture insert. Treated HUVECs (700 000 cells/mL) were suspended in ECM, and 70 μL of cell suspension aliquots were pipetted into each chamber of the cell culture insert. When the cell density reached more than 90% confluence, the culture insert was gently removed. Meanwhile, ECM was replaced with serum-free medium. Images were photographed using an inverted-phase microscope (IX51, OLYMPUS, Japan) 12 hours after a scratch was made in the cell monolayer. The reduction in the wounded area was measured with NIH ImageJ software (V.1.52a) and reported as a percentage.

Statistical analysis
Statistical analyses were accomplished using GraphPad Prism V.8.00 and R V.3.0. Statistical differences between two groups were analysed by using the unpaired Student's t-test, and those of differences among multiple groups of data were analysed by one-way analysis of variance.

RESULTS
The KRAS[G12D]-mutant induces the EndMT of HUVECs
Transcriptome differences between KRAS[G12D] mutant HUVECs (n=3) and control HUVECs (n=3) were evaluated by comparing the RNA-Seq expression profiles.
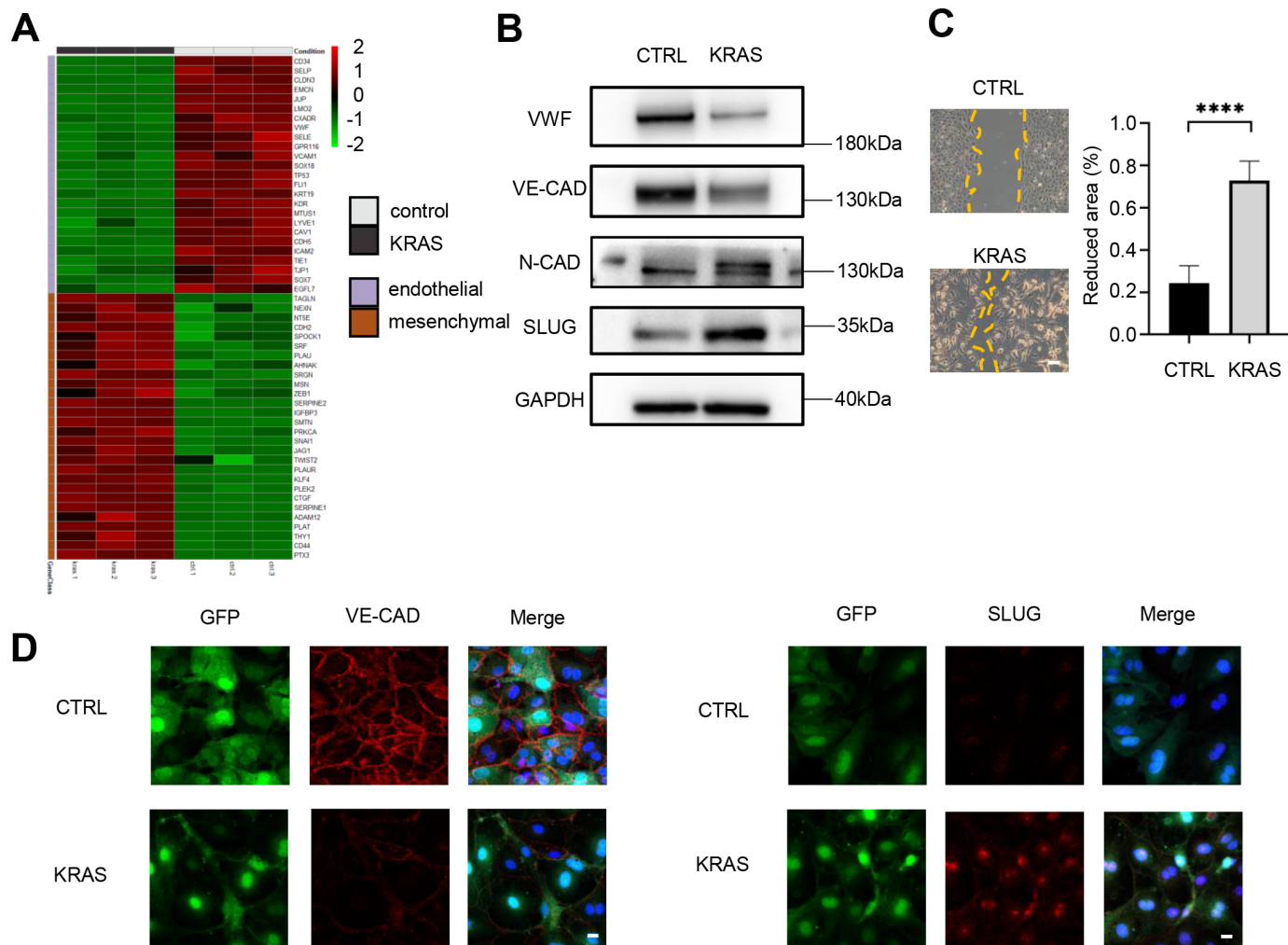
Figure 1 KRAS[G12D] mutation induces the EndMT of ECs. (A) Gene expression heatmap of differentially expressed endothelial and mesenchymal markers (p≤0.05 and fold change >1.50 or <0.67) in cell lines overexpressing the KRAS[G12D] mutant or a control virus in vitro. The x-axis shows HUVECs transfected with KRAS[G12D] or CTRL adenovirus (black=KRAS[G12D], grey=CTRL; n=3), and the y-axis shows individual genes. For the cells in the heatmap, red indicates high gene expression (ie, upregulated expression) relative to median expression; green indicates low expression (ie, downregulated expression); black indicates that the expression is similar to that of the median. (B) Western blot analysis of VE-cadherin, VWF, slug and N-cadherin in HUVECs subjected to different treatments. One result representative experiment of three is shown. (C) effects of the KRAS[G12D] mutant on HUVEC migration. The right panel shows the statistical analysis of the reduced area (n=6). One representative experiment of three experiments is shown. The scale bar corresponds to 100 µm. ****p<0.0001. (D) expression of VE-cadherin and Slug as determined by immunofluorescence staining. The GFP positive cells were HUVECs infected with KRAS[G12D] or control adenovirus. The results of one representative experiment of three experiments are shown. The scale bar corresponds to 100 µm. EndMT, endothelial-mesenchymal transition; HUVECs, human umbilical vein endothelial cells; VWF, von Willebrand factor.

Differentially expressed EndMT-related genes were defined as genes with an expression fold change>1.5 or <0.667 and a P≤0.05, and 53 genes were identified (online supplemental table S1). Compared with the control group, the expression of endothelial markers in the mutation group was significantly decreased, and the mesenchymal markers were increased (figure 1A). After infection with KRAS-mutant adenovirus, the mRNA levels of VWF and CDH5 were reduced, and those of CDH2 and SLUG were increased (online supplemental figure S1A). To further confirm that the EndMT in HUVECs was induced by KRAS mutation, we examined, in protein level by western blot analysis, the endothelial and mesenchymal markers. The results showed that the expression of VE-Cadherin and VWF was significantly downregulated, and N-Cadherin and SLUG were upregulated (figure 1B, online supplemental figure S2). Further investigation of cellular behaviour found that HUVECs infected with KRAS[G12D] adenovirus showed enhanced migration compared with the control HUVECs, and the cell morphology changed from polygonal to elongated shape, which is similar to mesenchymal cell phenotype. (figure 1C). Immunofluorescence staining revealed decreased expression of VE-Cadherin and increased expression of SLUG in HUVECs after treatment with KRAS[G12D] adenovirus (figure 1D). These results

suggested that the KRAS[G12D] mutant induced the EndMT of HUVECs.

Activation of the ERK-TGF-β/BMP signaling pathway, but not the Wnt or notch signaling pathway, contributes to KRAS mutant-induced EndMT

KRAS is an effector molecule that is expressed downstream of activated receptor tyrosine kinases and activates several pathways including the RAF-MEK - ERK pathway and the PI3K-AKT pathway.[15] In this study, the phosphorylation of ERK1/2, AKT, and p38 MAPK[16 17] was examined in HUVECs infected with KRAS[G12D] adenovirus. The increased level of ERK1/2 phosphorylation was observed in mutant KRAS expressing HUVECs, but not in AKT or p38 signalling pathways (figure 2A, online supplemental figure S3). U0126, a specific ERK inhibitor, inhibited the downregulation of endothelial marker expression, the upregulation of mesenchymal marker expression and the reduced cell mobility of KRAS[G12D]-mutant HUVECs (figure 2B–C, online supplemental figure S1B and figure S4). Our findings suggested that KRAS[G12D] mutant specifically activates the MAPK-ERK pathway in ECs.

Previous articles reported that the main pathways regulating the EndMT include the TGF-β, BMP, Notch and Wnt signalling pathways.[18–20] To determine which pathway downstream of KRAS regulates the EndMT, we focused on several key mRNAs and proteins related to the aforementioned signalling pathways. The TGF-β superfamily consists of more than 50 structurally related ligands that belong to three major subfamilies: TGF-beta, BMPs and Activins.[21] SMAD2 and 3 have been reported to be specifically activated by activin/nodal and TGF-β type I receptors, meanwhile SMAD1, 5 and 8 are activated by BMP type I receptors.[22] As shown in figure 2D and online supplemental figure S5, HUVECs infected with KRAS[G12D] adenovirus showed increased levels of p-SMAD2/3 and p-SMAD1/5, which was reversed by U0126, indicating that the TGF-β/BMP pathway is regulated by upstream ERK. Consistent with the results of the in vitro experiment, immunohistochemical staining of KRAS[G12D]-mutant cells in bAVM and superficial temporal artery tissues revealed that the levels of p-SMAD2/3 and p-SMAD1/5 were significantly increased in KRAS[G12D]-mutant bAVM tissue (online supplemental figure S6). Since the TGF-β and BMP pathways have similar biological effects in regulating the EndMT,[19 23] inhibiting only one of these pathways did not completely inhibit the EndMT. As shown in figure 2E and online supplemental figure S7, selective inhibition of the TGF-β pathway with the chemical inhibitor SB525334 or BMP pathway inhibitor LDN193189 only reversed the mesenchymal marker N-cadherin and SLUG.

To determine the effect on the Wnt signalling pathway, the total level of β-catenin in the HUVECs that undergone different treatment was measured by Western blotting. The results showed that KRAS mutant had no effect on total β-catenin expression. (figure 3A, online supplemental figure S8). In addition, the immunofluorescence assay indicated that the nuclear translocation of β-catenin was unchanged (figure 3B). These results suggested that the Wnt pathway was not activated. Examining the Notch signalling pathway, we found that KRAS[G12D] adenovirus transfection caused the mRNA levels of Notch2, Notch4, HEY1 and HEY2 to increase significantly (figure 3C). However, DAPT (a specific Notch pathway inhibitor[24] did not inhibit the EndMT, as measured at the protein level (figure 3D, online supplemental figure S9), suggesting that the Notch pathway was not associated with KRAS[G12D]-induced EndMT. In summary, the TGF-β and BMP signalling pathways played important roles in the KRAS[G12D]-induced EndMT, but the Wnt and Notch pathways had no effect on the EndMT

SMAD4 knockdown inhibits the EndMT in both KRAS[G12D]-mutant HUVECs and ECs of bAVMs

SMAD4 is a nuclear cofactor of Samd2/3 and SMAD1/5, and it can simultaneously regulate the TGF-β and BMP pathways.[25] We hypothesised that SMAD4 might be a core molecule in the KRAS-induced EndMT. To confirm the regulatory role of SMAD4 on the EndMT, we investigated changes in endothelial and mesenchymal markers expression in KRAS[G12D] mutant HUVECs in which SMAD4 was silenced. The gene knockdown efficiency of SMAD4 was confirmed by RT-qPCR (online supplemental figure S10). As displayed in figure 4A and online supplemental figure S11, N-Cadherin and SLUG expression was decreased, and that of VE-Cadherin and VWF was increased in cells with SMAD4 knocked down. Similarly, the immunofluorescence results were consistent with the Western blot results (online supplemental figure S12A). As shown in online supplemental figure S12B, SMAD4 knockdown in ECs partially reversed the fibroblast-like phenotype acquisition induced by KRAS[G12D], and the mobility of the cells was inhibited (n=9).

Primary ECs isolated from 3 bAVM surgical samples harbouring KRAS[G12D] somatic mutations were detected by WES. Through WES, we averaged 114×–217×coverage across the exome and obtained≥10× coverage and≥30× coverage for 95%–100% and 76%–85%, respectively (figure 4B). The results showed that all three cases of bAVM had KRAS[G12D] mutation in the endothelium (figure 4C, online supplemental figure S13). ddPCR also confirmed the presence of KRAS[G12D] mutation in bAVM primary cells.

In primary AVM ECs harbouring the KRAS[G12D] mutant, the expression of mesenchymal markers was decreased significantly after SMAD4 knockdown, but that of endothelial markers remained unchanged (figure 4D). The statistical analysis results are shown in online supplemental figure S14. This result may be explained by the fact that ECs undergoing the EndMT were excluded during CD31+magnetic bead sorting, and therefore, only ECs that partially exhibited mesenchymal behaviour were cultured. The results indicated that knockdown of SMAD4 expression inhibits the progression of EndMT in vitro.
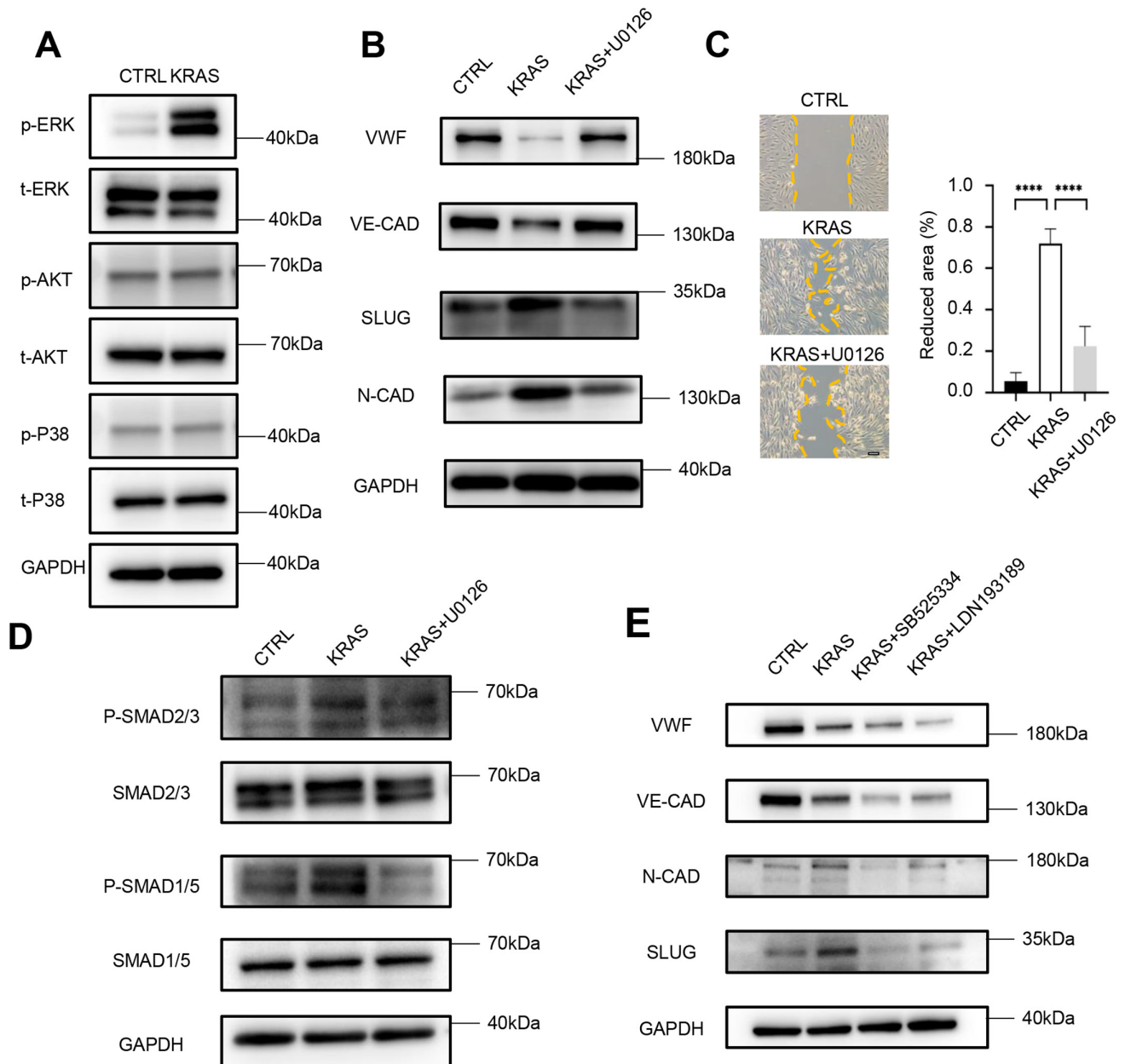
Figure 2 Activation of the ERK1/2-TGF-β/BMP signalling pathway contributes to the KRAS[G12D] mutation-induced EndMT. (A) HUVECs expressing KRAS[G12D] show elevated phosphorylated ERK1/2 levels, whereas no increases in phosphorylated Akt or phosphorylated p38 are detected. (B) Western blot showing the expression of mesenchymal markers N-cadherin and Slug, as well as that of endothelial markers VWF and VE-cadherin, in HUVECs overexpressing KRAS[G12D], HUVECs overexpressing KRAS[G12D] treated with U0126 and control HUVECs. Results from one representative experiment out of three are shown. (C) representative image of migration of HUVECs as determined by wound healing analysis (left). Scale bars: 100 μm. The right panel shows the statistical analysis of the reduced area (n=4). The T bars represent SD. (D) Western blot analysis of total Smad2/3, p-SMAD2/3, total Smad1/5, and p-SMAD1/5 in HUVECs exposed to KRAS[G12D] adenovirus, KRAS[G12D] adenovirus with U0126 (KRAS+U0126) or CTRL. The results of one representative experiment of three experiments are shown. (E) Western blot analysis of endothelial and mesenchymal markers in HUVECs subjected to different treatments. Result of one representative experiment of three experiments are shown. EndMT, endothelial-mesenchymal transition; HUVECs, human umbilical vein endothelial cells; VWF, von Willebrand factor.

Lovastatin attenuates the KRAS[G12D]-induced EndMT by inhibiting TGF-β/BMP pathway activation and SMAD4 acetylation

Lovastatin, as a lipid-lowering drug, inhibits the EndMT.[26] In this study, we found that lovastatin was able to restore the expression of VE-Cadherin and VWF that had been downregulated by KRAS[G12D] and that lovastatin reversed the upregulation of N-Cadherin and SLUG that had been induced by KRAS[G12D] (figure 5A, online supplemental figure S15). The results of immunofluorescence also confirmed that lovastatin reversed EndMT (online supplemental figure S16A). Moreover, lovastatin inhibited
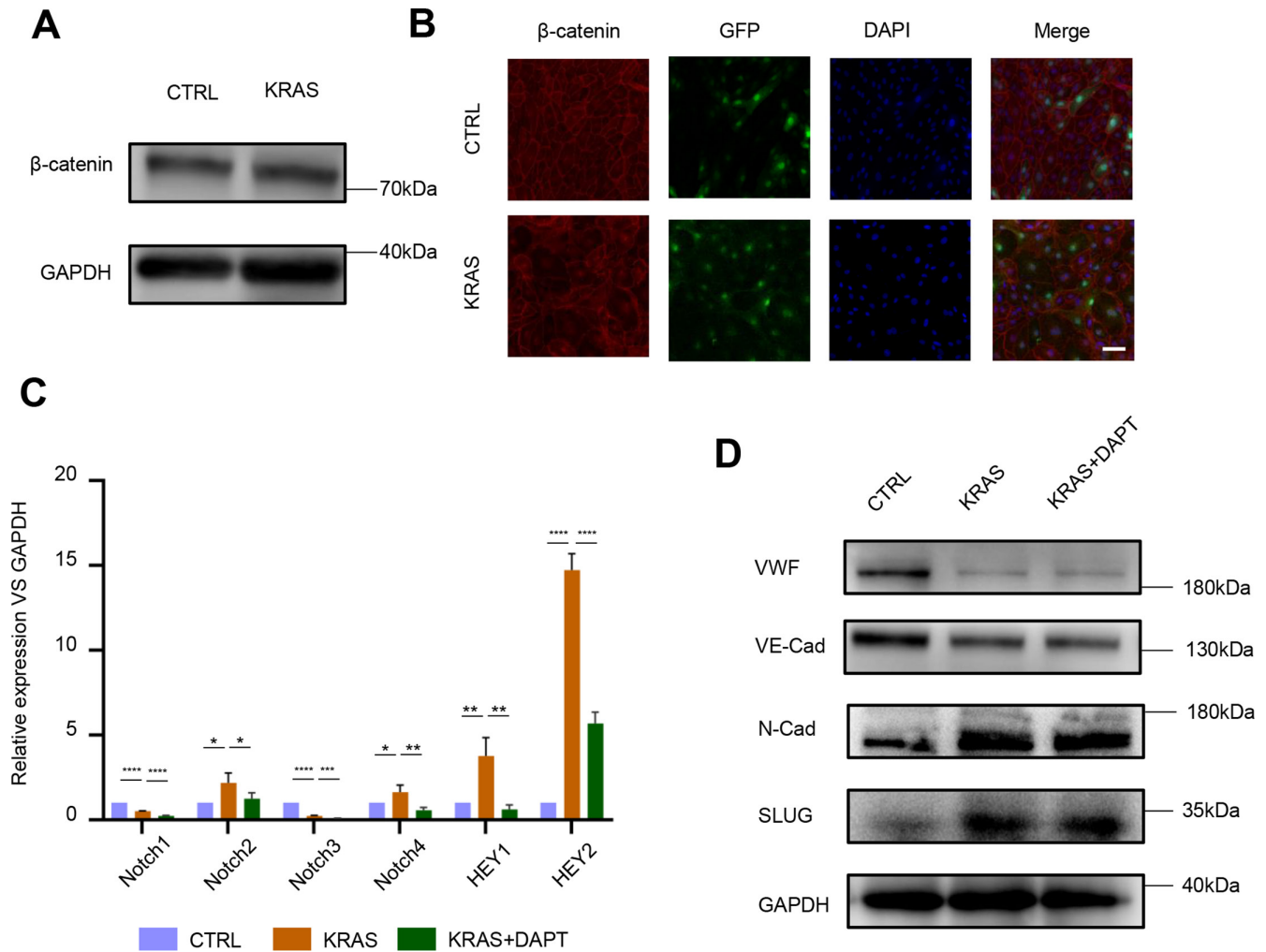
Figure 3 Wnt and Notch pathways are not involved in the KRAS[G12D]-induced EndMT. (A) Western blotting analysis of β-catenin expression in HUVECs infected with KRAS[G12D] adenovirus or negative control virus (CTRL). Results from one representative experiment out of three are shown. (B) immunofluorescence staining for β-catenin in HUVECs overexpressing KRAS[G12D] or negative control virus (CTRL). Results from one representative experiment out of three are shown. (C) RT-qPCR of Notch receptor (Notch1, 2, 3, 4) and HEY family gene (Hey1, 2) expression in HUVECs infected with KRAS[G12D] adenovirus or negative control virus (CTRL). *P value between groups was less than 0.05. (D), Western blot showing the expression of mesenchymal markers N-cadherin and Slug and endothelial markers VWF and VE-cadherin in HUVECs overexpressing KRAS[G12D], HUVECs overexpressing KRAS[G12D] treated with DAPT (a Notch pathway inhibitor) and control HUVECs (CTRL). Results from one representative experiment out of three are shown. EndMT, endothelial-mesenchymal transition; HUVECs, human umbilical vein endothelial cells; VWF, von Willebrand factor.

the increase in cell migration caused by the KRAS mutant (online supplemental figure S16B, n=9). In AVM ECs, lovastatin only reversed mesenchymal marker N-Cadherin and SLUG but not endothelial markers (online supplemental figure S16C).

To further investigate the mechanism by which lovastatin affects KRAS[G12D]-induced EndMT, we treated HUVECs infected with KRAS mutant adenovirus with lovastatin for 48 hours. First of all, we examined the effect of lovastatin on the TGF-β and BMP signalling pathways and found that lovastatin inhibited SMAD2/3 and SMAD1/5 phosphorylation (figure 5B, online supplemental figure S17). Then, we tested the effect of lovastatin on SMAD4, and the results showed no change in total SMAD4 expression (figure 5C, online supplemental figure S18).

A previous study has shown that TGF-β1 is able to increase acetylation level of SMAD4 to induce EndMT; SIRT1 inhibits this progress through deacetylating SMAD4.[23] As reported, SIRT1 is a nuclear NAD+-class III histone deacetylase, which influence their stability, transcriptional activity and translocation.[27] SIRT1 reportedly negatively regulated TGF-βpathway by targeting SMAD4,[28] and statins increased SIRT1 levels in ECs.[29] We hypothesised that this might be the molecular mechanism by which lovastatin inhibits EndMT induced by KRAS mutant. As shown in figure 5C and online supplemental figure S18, lovastatin increased the level of SIRT1 expression in HUVECs. Furthermore, we performed a coimmunoprecipitation assay to test the effect of lovastatin on SMAD4 acetylation. Our results showed that
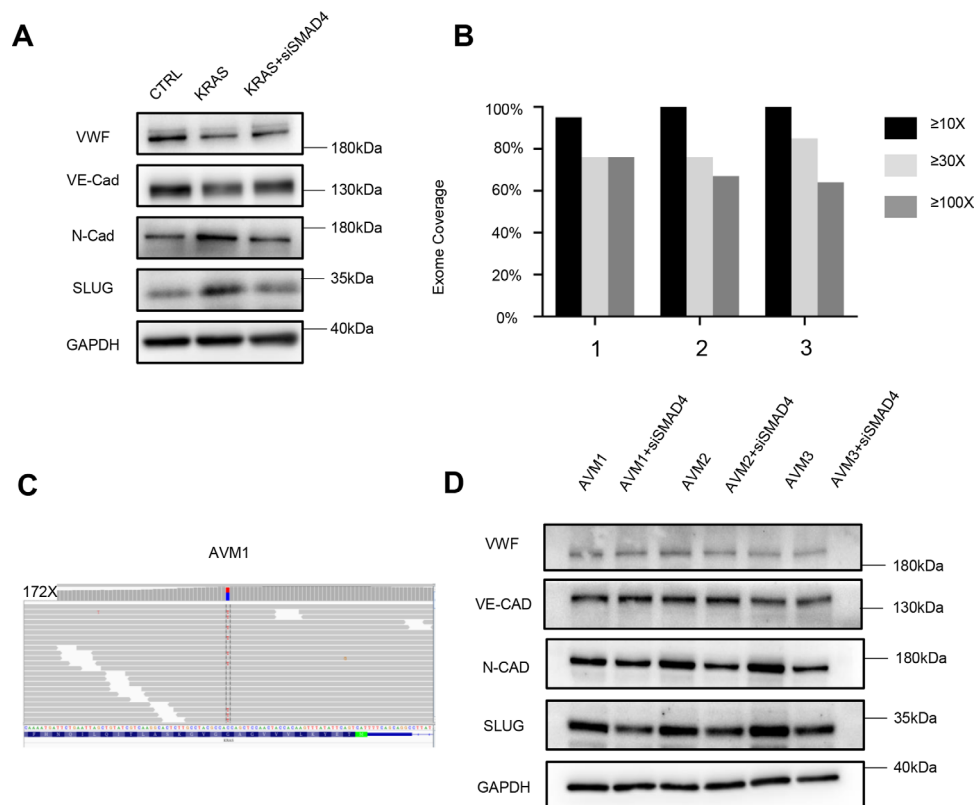
Figure 4 Knocking down Smad4 inhibits the EndMT in both KRAS[G12D]-mutant HUVECs and ECs in bAVM tissue. (A) Western blot showing the expression of mesenchymal markers N-cadherin and Slug and endothelial markers VWF and VE-cadherin in HUVECs overexpressing KRAS[G12D], HUVECs overexpressing KRAS[G12D] with siSMAD4 and control HUVECs (CTRL). Results from one representative experiment out of three are shown. (B) Bar graph indicating fold coverages across the exome for the bAVM ECs subjected to WES. ECs from participants yielded ≥100× coverage for ~90% of the exome. (C) Portion of an integrative genomic Viewer screen shot depicting WES coverage at the site of the KRAS[G12D] somatic missense mutation in participant1. The bar graph indicates the depth of coverage in the interval, which peaked at 172×. Colouring at the site of the mutation indicates the relative proportions of reference (blue) and variant (red) alleles in the sample. Examples of individual sequencing reads (horizontal grey bars) containing the variant and reference allele are depicted below. Note that the nine sequencing reads that contain the variant (T) allele are in both directions and have no other variant residues indicative of poor sequence quality or mismapping. (D) Western blot showing expression of mesenchymal markers and endothelial markers in KRAS[G12D]-mutant bAVM endothelial cells and SMAD4-knockdown cells. bAVMs, brain arteriovenous malformations; ECs, endothelial cells; EndMT, endothelial-mesenchymal transition; HUVECs, human umbilical vein endothelial cells; VWF, von Willebrand factor.

the acetylation levels of SMAD4 were upregulated in the KRAS[G12D]-mutant HUVECs and that lovastatin reduced the acetylation level of SMAD4 induced by KRAS[G12D] (figure 5D, online supplemental figure S19). Taken together, these results suggested that lovastatin inhibits the KRAS[G12D]-induced EndMT by inhibiting TGF-β/BMP pathway activation and SMAD4 acetylation.

DISCUSSION
In the current study, we found that KRAS mutation induces the EndMT by activating the ERK-TGF-β/BMP-SMAD4 pathway. Furthermore, we demonstrated that lovastatin inhibits the EndMT by inhibiting TGF-β/BMP pathway activation and SMAD4 acetylation.

The EndMT plays a crucial role in the occurrence and development of cardiovascular and cerebrovascular diseases,[30–32] and the reversal of the EndMT is becoming a promising treatment modality.[33 34] In bAVM tissue cells,

the EndMT is not only a pathogenic mechanism,[8] it is also closely associated with bAVM bleeding.[12] Our previous study demonstrated that the KRAS[G12D] mutant independently induced the EndMT. However, the mechanism by which KRAS mutations lead to the EndMT remains unclear. Previous studies reported that KRAS mutations lead to the activation of a wide range of downstream signalling pathways, including the TGF-β, BMP, Notch and Wnt pathways. In previous research, the activation of any of these pathways is independently capable of inducing the epithelial-mesenchymal transition (EMT) or EndMT.[18–20] In our study, we found that KRAS mutation induces the EndMT through the TGF-β/BMP-SMAD4 pathways but not the Wnt or Notch pathways and that knockdown of SMAD4 can reverse the EndMT process. Our results imply that SMAD4 may be a potential target by which to inhibit the development of bAVM with a KRAS mutant, an idea worthy of further research.
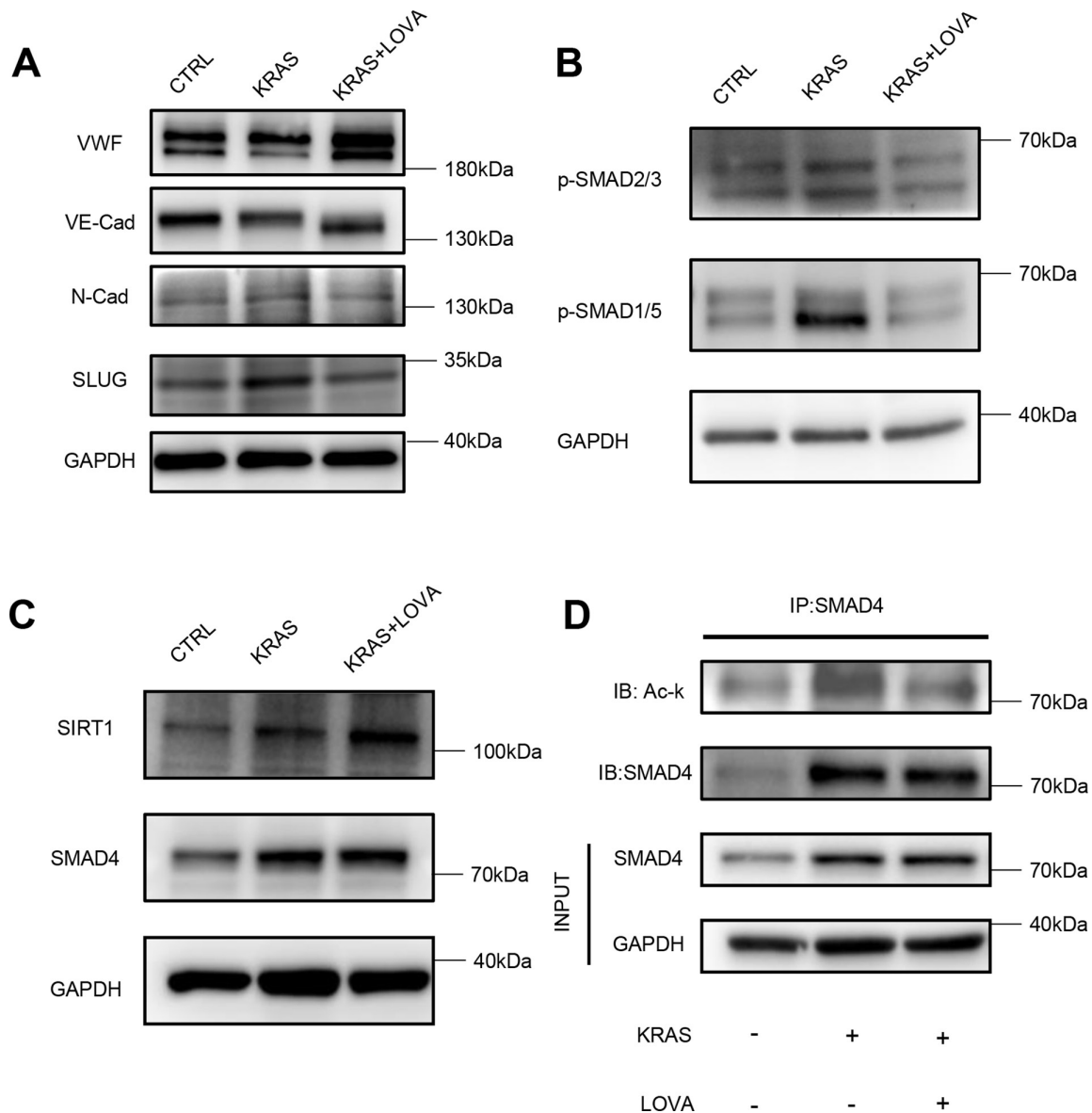
Figure 5 Lovastatin attenuates the KRAS^{G12D}-induced EndMT by inhibiting TGF-β/BMP pathway activation and Smad4 acetylation. (A) Western blot of mesenchymal markers N-cadherin and Slug and endothelial markers VWF and VE-cadherin in HUVECs overexpressing KRAS^{G12D}, HUVECs overexpressing KRAS^{G12D} with lovastatin and control HUVECs (CTRL). Results from one representative experiment out of three are shown. (B) Western blot showing the expression of p-SMAD2/3 and p-SMAD1/5 in HUVECs overexpressing KRAS^{G12D}, HUVECs overexpressing KRAS^{G12D} and treated with lovastatin and control HUVECs (CTRL). Results from one representative experiment out of three are shown. (C) Western blot of Smad4 and SIRT1 in KRAS^{G12D} HUVECs, KRAS^{G12D} HUVECs treated with lovastatin and CTRL. Results from one representative experiment out of three are shown. (D) Immunoprecipitation of Smad4 acetylation after lovastatin treatment. Results from one representative experiment out of three are shown. EndMT, endothelial-mesenchymal transition; HUVECs, human umbilical vein endothelial cells; VWF, von Willebrand factor.

Lovastatin is an Food and Drug Administration (FDA)-approved drug that has been used widely as a lipid-lowering medication[35] and has also been reported to reverse the EndMT; the mechanism of lovastatin action might involve the suppression of oxidative stress and inhibited TGF-β1/SMAD signalling pathway activation.[26] Our previous study demonstrated that lovastatin inhibits the EndMT caused by a KRAS mutant. In the current study, we found that lovastatin has the ability to inhibit the TGF-β/BMP pathway and decrease SMAD4 acetylation to attenuate the KRAS^{G12D}-induced EndMT. In summary, lovastatin, as a novel pharmacological target, may alleviate the development of bAVMs and reduce the risk of bAVM rupture; therefore, further exploration of lovastatin treatment in animal studies and clinical trials is needed.h

ORCID iDs
Yuming Jiao http://orcid.org/0000-0001-8351-4602
Qiheng He http://orcid.org/0000-0001-6715-298X
Yong Cao http://orcid.org/0000-0002-8289-1120

REFERENCES

1 Lawton MT, Rutledge WC, Kim H, *et al*. Brain arteriovenous malformations. *Nat Rev Dis Primers* 2015;1:15008.
2 Goss JA, Huang AY, Smith E, *et al*. Somatic mutations in intracranial arteriovenous malformations. *PLoS One* 2019;14:e0226852.
3 Mohr JP, Parides MK, Stapf C, *et al*. Medical management with or without Interventional therapy for unruptured brain arteriovenous malformations (ARUBA): a multicentre, non-blinded, randomised trial. *Lancet* 2014;383:614–21.
4 Nikolaev SI, Vetiska S, Bonilla X, *et al*. Somatic activating KRAS mutations in arteriovenous malformations of the brain. *N Engl J Med* 2018;378:250–61.
5 Hong T, Yan Y, Li J, *et al*. High prevalence of KRAS/BRAF somatic mutations in brain and spinal cord arteriovenous malformations. *Brain* 2019;142:23–34.
6 Fish JE, Flores Suarez CP, Boudreau E, *et al*. Somatic gain of KRAS function in the endothelium is sufficient to cause vascular malformations that require MEK but not PI3K signaling. *Circ Res* 2020;127:727–43.
7 Park ES, Kim S, Huang S, *et al*. Selective endothelial hyperactivation of oncogenic KRAS induces brain arteriovenous malformations in mice. *Ann Neurol* 2021;89:926–41.
8 Li H, Nam Y, Huo R, *et al*. De novo germline and somatic variants convergently promote endothelial-to-mesenchymal transition in simplex brain arteriovenous malformation. *Circ Res* 2021;129:825–39.
9 Dejana E, Hirschi KK, Simons M. The molecular basis of endothelial cell plasticity. *Nat Commun* 2017;8:14361.
10 Man S, Sanchez Duffhues G, Ten Dijke P, *et al*. The therapeutic potential of targeting the endothelial-to-mesenchymal transition. *Angiogenesis* 2019;22:3–13.
11 Yao J, Wu X, Zhang D, *et al*. Elevated endothelial Sox2 causes lumen disruption and cerebral arteriovenous malformations. *J Clin Invest* 2019;129:3121–33.
12 Fu W, Huo R, Yan Z, *et al*. Mesenchymal behavior of the endothelium promoted by Smad6 downregulation is associated with brain arteriovenous malformation microhemorrhage. *Stroke* 2020;51:2197–207.
13 Li H, Durbin R. Fast and accurate long-read alignment with burrows-wheeler transform. *Bioinformatics* 2010;26:589–95.
14 Li H, Handsaker B, Wysoker A, *et al*. The sequence alignment/Map format and SAMtools. *Bioinformatics* 2009;25:2078–9.
15 Yan C, Theodorescu D. Ral GTPases: biology and potential as therapeutic targets in cancer. *Pharmacol Rev* 2018;70:1–11.
16 Lim JKM, Leprivier G. The impact of oncogenic ras on redox balance and implications for cancer development. *Cell Death Dis* 2019;10:955.
17 Hill KS, Erdogan E, Khoor A, *et al*. Protein kinase Cα suppresses KRAS-mediated lung tumor formation through activation of a p38 MAPK-TGFβ signaling axis. *Oncogene* 2014;33:2134–44.
18 Cooley BC, Nevado J, Mellad J, *et al*. TGF-β signaling mediates endothelial-to-mesenchymal transition (EndMT) during vein graft remodeling. *Sci Transl Med* 2014;6:227ra34.
19 Maddaluno L, Rudini N, Cuttano R, *et al*. EndMT contributes to the onset and progression of cerebral cavernous malformations. *Nature* 2013;498:492–6.
20 Chang ACY, Fu Y, Garside VC, *et al*. Notch initiates the endothelial-to-mesenchymal transition in the atrioventricular canal through autocrine activation of soluble guanylyl cyclase. *Dev Cell* 2011;21:288–300.
21 Feng X-H, Derynck R. Specificity and versatility in TGF-beta signaling through smads. *Annu Rev Cell Dev Biol* 2005;21:659–93.
22 Two major Smad pathways in TGF- β superfamily signalling
23 Gonzalez DM, Medici D. Signaling mechanisms of the epithelial-mesenchymal transition. *Sci Signal* 2014;7:re8.
24 Feng J, Wang J, Liu Q, *et al*. Dapt, a γ-secretase inhibitor, suppresses tumorigenesis, and progression of growth hormone-producing adenomas by targeting notch signaling. *Front Oncol* 2019;9:809.
25 Park D-S, Yoon G-H, Kim E-Y, *et al*. Wip1 regulates SMAD4 phosphorylation and inhibits TGF-β signaling. *EMBO Rep* 2020;21:e48693.
26 Ma Z, Zhu L, Liu Y, *et al*. Lovastatin alleviates endothelial-to-mesenchymal transition in glomeruli via suppression of oxidative stress and TGF-β1 signaling. *Front Pharmacol* 2017;8:473.
27 Potente M, Ghaeni L, Baldessari D, *et al*. SIRT1 controls endothelial angiogenic functions during vascular growth. *Genes Dev* 2007;21:2644–58.
28 Chen I-C, Chiang W-F, Huang H-H, *et al*. Role of SIRT1 in regulation of epithelial-to-mesenchymal transition in oral squamous cell carcinoma metastasis. *Mol Cancer* 2014;13:254.
29 Singh I, Samuvel DJ, Choi S, *et al*. Combination therapy of lovastatin and AMP-activated protein kinase activator improves mitochondrial and peroxisomal functions and clinical disease in experimental autoimmune encephalomyelitis model. *Immunology* 2018;154:434–51.
30 Kovacic JC, Dimmeler S, Harvey RP, *et al*. Endothelial to mesenchymal transition in cardiovascular disease: JACC state-of-the-art review. *J Am Coll Cardiol* 2019;73:190–209.
31 Chen D, Li L, Wang Y, *et al*. Ischemia-reperfusion injury of brain induces endothelial-mesenchymal transition and vascular fibrosis via activating let-7i/TGF-βR1 double-negative feedback loop. *Faseb J* 2020;34:7178–91.
32 Shoemaker LD, McCormick AK, Allen BM, *et al*. Evidence for endothelial-to-mesenchymal transition in human brain arteriovenous malformations. *Clin Transl Med* 2020;10:e99.
33 Zeisberg EM, Tarnavski O, Zeisberg M, *et al*. Endothelial-to-mesenchymal transition contributes to cardiac fibrosis. *Nat Med* 2007;13:952–61.
34 Cho JG, Lee A, Chang W, *et al*. Endothelial to mesenchymal transition represents a key link in the interaction between inflammation and endothelial dysfunction. *Front Immunol* 2018;9:294.
35 Liu B, Zhang X, Zhang W, *et al*. Lovastatin inhibits HIV-1-induced MHC-I downregulation by targeting nef-AP-1 complex formation: a new strategy to boost immune eradication of HIV-1 infected cells. *Front Immunol* 2019;10:2151.